Shedding Light on the Molecular Surface Assembly at the Nanoscale Level: Dynamics of a Re(I) Carbonyl Photosensitizer with a Co-adsorbed Cobalt Tetrapyridyl Water Reduction Catalyst on ZrO_2

Kerstin Oppelt*, Mathias Mosberger, Jeannette Ruf, Ricardo Fernández-Terán, Benjamin Probst, Roger Alberto and Peter Hamm*

Department of Chemistry, University of Zurich. Winterthurerstrasse 190, Zurich, Switzerland.

SUPPORTING INFORMATION

Contents

List of Compounds 2

Abbreviations 2

Experimental Details and Synthesis 4

- Chemicals and Characterization Methods 4
- Synthesis of Re(I) Tricarbonyl Complexes 6
- Synthesis of Organic Compounds 6
- Synthesis of Co(II) Tetrapyridyl Complexes 8
- Adsorption of Molecules on Mesoporous Metal Oxides 9
- Quantification of the Adsorbed Species 9

Time Resolved Measurements 11

- Experimental Methods 11
- tr-IR Results 12

FT-IR Measurements 15

Electrochemical Measurements 17

References 18

List of Compounds

1. [ReClPAbpy$(CO)_3$]
2. [Re(py)PAbpy$(CO)_3$] OTf

11. 3,5-Bis((diethoxyphosphoryl)methyl)-benzyl alcohol
12. 3,5-Bis((diethoxyphosphoryl)methyl)-benzyl bromide
13. Di(4-methyl-2-pyridyl)methanone
14. [2,2'-Bipyridin]-6-ylbis(4-methylpyridin-2-yl)methanol DMTPy
15. DMTPy-O-Benzyl-3,5-bis($MePO_3Et_2$) $BisPod^{Et}$
16. DMTPy-O-Benzyl-3-($MePO_3H_2$)-5-($MePO_3HNa$) $BisPod^{H}$

20. [$CoBr_2$(TPy-OH)]
21. [$CoBr_2$(DMTPy-O-Benzyl-3,5-bis($MePO_3Et_2$))] $Co^{II}BisPod^{Et}$
22. [Co(DMTPy-O-Benzyl-3,5-bis($MePO_3H$)] $Co^{II}BisPod^{H}$

Abbreviations

aq.	aqueous
CH_2Cl_2	dichloromethane
Et_2O	diethylether
EtOAc	ethylacetate
HV	high vacuum
MeOH	methanol
org.	organic
-OTf	trifluoromethanesulfonate anion
sat.	saturated
THF	tetrahydrofuran
NPs	nanoparticles

Re(I) Tricarbonyl Complexes

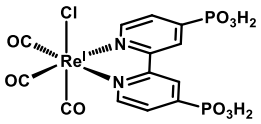

1, PS

$^{Cl}Re^{PAbpy}$

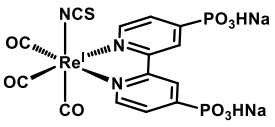

2

$^{NCS}Re^{PAbpy}$

Organic Compounds

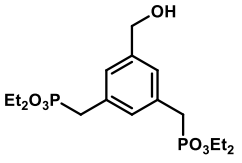

11

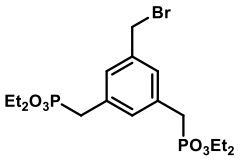

12

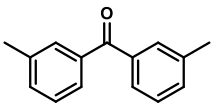

13

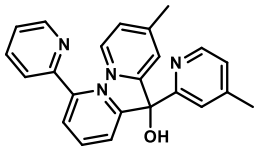

14

DMTPy

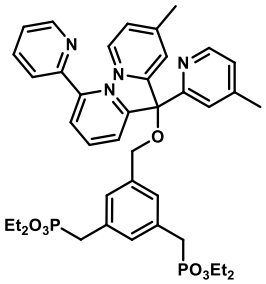

15

$BisPod^{Et}$

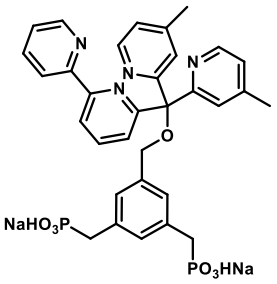

16

$BisPod^{H}$

Co(II) Tetrapyridyl Complexes

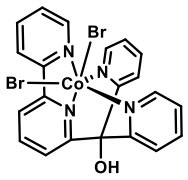

20

$CoBr_2(TPy\text{-}OH)$

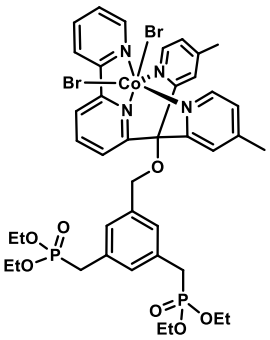

21

$Co^{II}BisPod^{Et}$

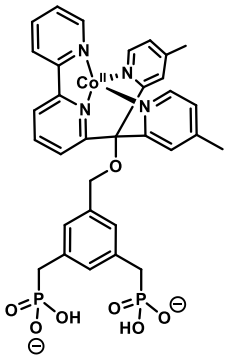

22, WRC

$Co^{II}BisPod^{H}$

Scheme S 1 Compound Overview

Experimental Details and Synthesis

Chemicals and Characterization Methods

Chemicals were of reagent grade and used without further purification if not indicated. Cobalt(II) bromide ($CoBr_2$) was obtained from *Acros*, tetrabromomethane (CBr_4) from *Apollo*, pyridine (py) and Zinc(II) chloride ($ZnCl_2$) from *Fluka,* methyl 3,5-dimethylbenzoate from *Fluorochem* whereas 2-bromo-6-(pyridin-2-yl)pyridine was purchased from *PCNS*, bromotrimethylsilane (TMSBr), dry MeOH, *n*-Butyllithium solution (*n*BuLi, 1.6 M in hexane), potassium *tert*-butoxide (KO*t*Bu), silver trifluoromethanesulfonate (AgOTf), triphenylphosphine (PPh_3), 1,3,5-tris(bromomethyl)benzene (TBM) were acquired from *Sigma Aldrich* and trifluoromethanesulfonic acid (HOTf) from *TCI*. Ascorbate, ascorbic acid and phenothiazine derivatives were purchased from commercial suppliers.

Reactions were carried out under N_2 in oven-dried (120 °C) glass equipment and monitored for completion by analysing a small sample (after suitable workup) by HPLC or UPLC/ESI-MS. Solvents for synthesis were of analysis grade, whereas for workup, distilled technical grade solvents were used. Dry CH_2Cl_2 was dispensed from a *MBRAUN* SPS-system, and dry Et_2O and THF was obtained by distillation over metallic sodium.

Evaporation of the solvents *in vacuo* was done with the rotary evaporator at the given bath temperature and pressure and drying was done at high vacuum (HV) using a Schlenk-line. pH: *Merck* indicator paper pH 1–14 (universal indicator). Automated flash chromatography was performed on an *Argonaut* Flash Master using self-packed reversed phase C18-silica gel (C18 silica gel spherical from *Sigma Aldrich*) columns with the indicated solvent system. Columns were properly flushed with MeOH before and after use. Purification or desalination by Sep-Pak® Cartridges from *Waters* was done according to the description with the given solvent system. Cartridges were activated with MeOH (6 mL) and then flushed with H_2O (10 mL) before loading.

UV/Vis spectra were measured on a *Analytik Jena Specord 250 Plus* with solution samples in 1 cm quartz cell, sensitized oxide films and the spectroelectrochemistry were measured with a Shimadzu UV 2450 (PC) Spectrometer.

Emission measurements were performed on an *Edinburgh Instrument FLS900* fluorescence spectrometer with argon-purged sample solutions (0.1 mM) in the indicated solvent in a 1 cm cell.

Emission lifetime measurements were also carried out on *Edinburgh Instrument FLS900* fluorescence spectrometer using an EPL-Laser (picosecond pulsed diode laser) for excitation and a cooled micro-channel plate photomultiplier (MCP-PMT) for single photon counting. Samples were measured as nitrogen-purged sample solutions in 1 cm quartz cells.

IR spectra were recorded on a *Perkin Elmer Spectrum Two FT-IR spectrometer* with neat solid samples (ATR). Abbreviations used in the description of the FT-IR data are as follows: w, weak; m, middle; s, strong. The sensitized oxide films on CaF_2 were measured in transmission with a Bruker Tensor 27 spectrometer.

^{1}H-NMR spectra were measured at 298 K in the indicated solvent on a *Bruker AV-400* (400 MHz); δ in ppm rel. to the signal of the indicated solvent (δ=7.26 ppm ($CDCl_3$), 2.5 ppm ($(CD_3)_2SO$); δ= 0 corresponds to TMS), *J* in Hz.

Abbreviations used in the description of NMR data are as follows: s, singlet; d, doublet; t, triplet; q, quartet; p, quintet; m, multiplet.

^{13}C-NMR spectra were measured at 298 K in the indicated solvent; *Bruker AV-400* (100 MHz); δ in ppm rel. to the indicated solvent ($CDCl_3$ (δ=77.0), MeOD (δ=49.0)); multiplicities from DEPT-135 and DEPT-90 experiments.

^{31}P-NMR spectra were measured at 298 K in the indicated solvent; *Bruker AV-400* (162 MHz).

^{19}F-NMR spectra were measured at 298 K in the indicated solvent on a *Bruker AV-400* (376 MHz).

HPLC-3 measurements were performed on a *Chromemaster VWR Hitachi* using a *Nucleodur C18 gravity column* operated in an oven (5310) at 40 °C and a *PDA detector* (5430). The gradient was as follows: A = 0.1 % FA in H_2O; B = MeCN; flow rate 1.5 mL min^{-1}; 0.0–5.8 min 5–100 % B; 5.8–6.8 min 100 % B; 6.8–7.3 min 0–90 % A; 7.3–9.5 min 90 % A.

UPLC/ESI-MS: UPLC separation was performed on an *Acquity™ Ultra Performance LC* with an *Acquity UPLC® BEH C18 column* (1.7 µm, 2.1 × 50 mm; 0.5 mL/min flow rate) and a gradient of 0.1% aqueous formic acid and acetonitrile eluents. Mass spectra were recorded on an *Esquire HCT from Bruker* (Germany), the injection rate was 3 µL/min, the nebulizer pressure was 10 psi, and the dry gas flow rate was 5 L/min at 350 °C. All solvents were of HPLC/LCMS grade and water was doubly-distilled.

High-resolution electrospray mass spectra (HR-ESI-MS) were recorded on a maXis QTOF-MS instrument (*Bruker Daltonics GmbH*, Bremen, Germany). The samples were dissolved in (e.g. MeOH) at a concentration of ca. 50 µg/ml and analyzed via continuous flow injection (2 µL/min). The mass spectrometer was operated in the positive (or negative) electrospray ionization mode at 4'000 V (-4'000 V) capillary voltage, -500 V (500 V) endplate offset, with a N_2 nebulizer pressure of 0.8 bar and dry gas flow of 4 l min^{-1} at 180°C. Mass spectra were acquired in the mass range from m/z 50 to 2'000 at 20'000 resolution (full width at half maximum) and 1.0 Hz rate. The mass analyzer was calibrated between m/z 118 and 2721 using an Agilent ESI-L low concentration tuning mix solution (Agilent, USA) at a resolution of 20'000 and a mass accuracy below 2 ppm. All solvent used were purchased in best LC- MS qualities.

Elemental analysis was carried out on a *LECO Truespec CHNS(O)* microanalyzer; calculated with *ChemDrawPro 16*.

ICP-MS measurements were performed with an *Agilent* QQQ 8800 Triple quad ICP-MS spectrometer, equipped with a standard x-lens setting, nickel cones and a "micro-mist" quartz nebulizer. The feed was 0.1 ml/min, the RF power 1550 W. Tune settings were based on the *Agilent* General Purpose method and only slightly modified by an autotune procedure using an Agilent 1 ppb tuning solution containing Li, Y, Ce and Tl. Values are reported as the average of 30 sweeps x 3 replicates. Elements were measured in a "helium-mode". The name is referring to the gas in the reaction cell. All solutions were prepared from 30% HCl (*Merck* 1.01514.1000 ultrapure) and 18.2 MΩ Millipore water. Elements were measured against a serial dilution made with the following standards: Cobalt: *Merck* 1.70313.0100 in 2% HNO_3, Rhenium: *Merck* 1.70344.0100 in H_2O, Indium: *Merck* 1.70324.0100 in 2% HNO_3 as internal standard.

To the solid samples, 30% HCl (0.7 mL) and Millipore water (3 mL) were added and the mixtures were ultrasonicated for 2.5 h. Additional 30% HCl were added and further treated in the ultrasonic bath for 3 days until everything was dissolved. Volumes were filled up to 10 mL and diluted 1:10 with 7% HCl. Calibration measurements

(0/0.25/0.5/1/5/10/50/100/250/500 ng/mL Co, Re in 7% HCl) were carried out and the metal concentrations (given in ng/mL) of the diluted sample solutions were determined. All measurement and calibration solutions contained 100 ng/mL In in 7% HCl as internal standard.

Cyclic Voltammetry of **PS** in aqueous solution with 0.1 M KCl was performed using an Ivium Vertex potentiostat with a with a glassy carbon working electrode, Pt auxiliary electrode and Ag/AgCl/3M NaCl reference electrode, all from BASI. Electrochemical Analysis of $CoBr_2$(tpy-OH) **20** was performed in H_2O with lithium trifluoromethanesulfonate (0.1 M) as electrolyte on glassy carbon, with a Pt auxiliary electrode and an Ag/AgCl reference electrode with a Metrohm 797 VA Computrace. Potassium ferricyanide was used as internal standard.

Spectroelectrochemistry of the **ED** N-methyl-phenothiazine was performed with an OTTLE cell[1] with a Pt grid working electrode, Pt auxiliary electrode and Ag wire quasi reference electrode using an Ivium Vertex potentiostat. The samples were dissolved in acetonitrile-d_3 with $TBABF_4$ as conducting electrolyte. A set off constant potentials was applied at the working electrode and after the initial current had equilibrated the UV/Vis absorption spectra were recorded. The potential at the working electrode was calibrated externally against the ferrocene/ ferrocenium redoxpair.

Synthesis of Re(I) Tricarbonyl Complexes

[Re(Cl)(PAbpy)$(CO)_3$] (**PS**)[2] and [Re(NCS)(PAbpy)$(CO)_3$] (**2**) were synthesized according to published procedures.[3]

Synthesis of Organic Compounds

3,5-Bis((diethoxyphosphoryl)methyl)-benzyl alcohol (**11**)[4,5] and di(4-methyl-2-pyridyl)methanone (**13**)[6] were prepared according to published procedures. 3,5-Bis((diethoxyphosphoryl)methyl)-benzyl bromide (**12**) was synthesized by modifying a literature procedure of Cooray and co-workers.[7,8]

3,5-Bis((diethoxyphosphoryl)methyl)-benzyl bromide (**12**)[7,8]: A solution of benzyl alcohol **11** (167 mg, 0.409 mmol) and CBr_4 (149 mg, 0.450 mmol, 1.1 eq.) in CH_2Cl_2 (1 mL) was stirred under N_2 and cooled to 0 °C using an ice bath. PPh_3 (118 mg, 0.450 mmol, 1.1 eq.) was dissolved in CH_2Cl_2 (1.5 mL) and added to the cooled solution, which was further stirred at 0 °C under N_2. When reaction control showed full consumption of **11**, the mixture was diluted with $CHCl_3$ (10 mL) and the org. phase was washed with sat. aq. Na_2CO_3 (2 x 10 mL), brine (2 x 10 mL) and H_2O (2 x 10 mL). The org. phase was then dried over Na_2SO_4, filtered, concentrated in vacuo (42 °C, 400 mbar) and dried at HV, which delivered crude **12** (387 mg). To remove $OPPh_3$ from the mixture, crude was dissolved in EtOAc (1.05 mL) and dry $ZnCl_2$ (112 mg, 0.819 mmol, 2 eq.) was added. After stirring the suspension for 6 h at 23 °C, the formed precipitate was filtered off and rinsed with additional EtOAc (1 mL). Solvent was removed in vacuo (42 °C, 200 mbar) and the residue was dried at HV to obtain **12** (224 mg, 0.401 mmol, 85 wt%) as an off-white solid in a yield of 98%. ^{1}H-NMR (400 MHz, $CDCl_3$): δ 7.23 (d, J = 1.9 Hz, 2 H); 7.16 (s, 1 H); 4.45 (s, 2 H); 4.02 (p, J = 7.2 Hz, 8 H); 3.12 (d, J =

21.9 Hz, 4 H); 3.12 (d, J = 21.9 Hz, 12 H). ^{31}P-NMR (162 MHz, MeOD) δ 25.70. UPLC/ESI-MS (r_t = 2.4 min): m/z = 473.1 (100, $[M+H]^+$).

*[2,2'-bipyridin]-6-ylbis(4-methylpyridin-2-yl)methanol (**14**, DMTPy):* To a stirred solution of 2-bromo-6-(pyridin-2-yl)pyridine (1.55 g, 6.58 mmol) in dry Et_2O (80 mL), *n*BuLi solution (1.6 M in hexane, 4.2 ml, 6.58 mmol) was added dropwise. The rate was adjusted as such, that the reaction mixture never exceeded -95 °C. After stirring for 1 h, a solution of di(4-methyl-2-pyridyl)methanone (13, 1.33 g, 6.25 mmol) in dry THF (25 mL) was added dropwise while keeping the temperature below -95 °C. The reaction was allowed to warm to 60 °C, which was then quenched with MeOH (0.5 mL) and concentrated *in vacuo* (42 °C, 280 mbar). The brown oily residue was taken up in diluted aqueous K_2CO_3 (300 mL) and extracted with CH_2Cl_2 (3 x 300 mL). The combined organic phases were dried over $MgSO_4$, concentrated *in vacuo* (42 °C, 680 mbar) and dried at HV. Recrystallization from boiling Et_2O gave pure **14** (1.05 g, 2.85 mmol) as beige solid in a yield of 43%. ^{1}H-NMR (400 MHz, $CDCl_3$): δ 8.64 (ddd, *J* = 4.8, 1.8, 0.9 Hz, 1 H); 8.42 (dd, *J* = 5.0, 0.4 Hz, 2 H); 8.33 (dd, *J* = 7.6, 1.2 Hz, 1 H); 8.20 (dt, *J* = 8.0, 1.0 Hz, 1 H); 7.82 (t, *J* = 7.7 Hz, 1 H); 7.77 – 7.69 (m, 2 H); 7.58 (p-like s, *J* = 0.8 Hz, 2 H); 7.34 (s, 1 H); 7.25 (d, *J* = 7.5, 4.8, 1.2 Hz, 1 H); 7.01 (ddd, *J* = 5.0, 1.6, 0.7 Hz, 2 H); 2.32 (s, 6 H). UPLC/ESI-MS (r_t = 1.7 min): *m/z* = 276.1 (2, $[M–C_6H_6N]^+$), 369.3 (100, $[M+H]^+$).

*DMTPy-O-Benzyl-3,5-bis(MePO$_3$Et$_2$) (**15**, BisPod^{Et}):* A suspension of DMTPy (**14**, 50 mg, 0.136 mmol) and KO*t*Bu (31 mg, 0.272 mmol, 2 eq.) in dry THF (3 mL) was stirred for 10 min at 23 °C under N_2 and was then added dropwise to a solution of compound **12** (622 mg, 1.32 mmol, 8.2 eq.) in dry THF (3.0 mL) leading to a colour change of the reaction mixture to yellowish. Additional KO*t*Bu (153 mg, 1.360 mmol, 10 eq.) was added in portions of 1 eq. until full consumption of **12** was observed. After the reaction was quenched with MeOH (4 mL), the reaction mixture was poured on aq. HCl (0.1 M, 30 mL) and the milky aq. phase was washed with CH_2Cl_2 (3 x 40 mL). After basifying using sat. aq. Na_2CO_3 and extraction with CH_2Cl_2 (3 x 40 mL), the org. phases were combined, dried over Na_2SO_4, filtered, concentrated *in vacuo* (42 °C, 680 mbar) and dried at HV to obtain crude **15** (55 mg) as a sticky light brownish solid. Purification by automated column chromatography (C18 silica, H_2O/MeOH 7:3 to 0:10) delivered pure fractions, which were combined, MeOH was removed *in vacuo* (42 °C, 100 mbar) and the aqueous phase was extracted with CH_2Cl_2 (3 x 50 mL). Combined org. phases were dried over Na_2SO_4, filtered, solvent removed *in vacuo* (42 °C, 680 mbar) and dried at HV to obtain pure **15** (17 mg, 0.022 mmol, 17 %) as a colourless viscous oil in >95% purity according to ^{1}H-NMR.

^{1}H-NMR (400 MHz, $CDCl_3$): δ 8.62 (ddd, *J* = 4.8, 1.8, 0.9 Hz, 1 H); 8.45 (d, *J* = 4.9 Hz, 2 H); 8.28 (dd, *J* = 7.8, 1.0 Hz, 1 H); 8.13 (dt, *J* = 8.0, 1.1 Hz, 1 H); 7.77 (t, *J* = 7.8 Hz, 1 H); 7.67 (td, *J* = 7.9, 1.8 Hz, 1 H); 7.62 (dd, *J* = 7.9, 1.0 Hz, 1 H); 7.59 (p-like s, *J* = 0.8 Hz, 1 H); 7.23 (ddd, *J* = 7.5, 4.8, 1.2 Hz, 1 H); 7.20 (q-like s, *J* = 1.9 Hz, 2 H); 7.12 (s, 1 H); 6.99 (d, *J* = 4.7 Hz, 2 H); 4.56 (s, 2 H); 3.98 (p, *J* = 7.1 Hz, 8 H); 3.10 (d, *J* = 21.8 Hz, 4 H); 2.33 (s, 6 H); 1.20 (t, *J* = 7.1 Hz, 12 H). ^{31}P-NMR (162 MHz, $CDCl_3$): δ 26.34. ^{13}C-NMR (100 MHz, $CDCl_3$): δ 161.14 (2s), 160.44 (s), 156.25 (s), 154.44 (s), 148.95(2d), 148.01(2s), 147.83(d), 139.75 (s), 137.23 (d), 137.07 (d), 131.83 (2s), 130.15 (d), 127.81 (2d), 125.22 (2d), 124.59 (d), 123.70 (2d), 123.61 (d), 121.55 (d), 119.58 (d), 88.19 (s), 67.17 (t), 62.22 (4t), 34.36 (t), 32.99 (t), 21.55 (2q), 16.53(4q). UPLC/ESI-MS (r_t = 2.4 min): 380.2 (100, $[M+2H]^{2+}$), 759.3 (4, $[M+H]^+$). HPLC-3: r_t = 3.55 min. HR-ESI-MS (MeOH): 759.30609 (100, $C_{40}H_{49}N_4O_7P_2^+$; $[M+H]^+$; calc. 759.30710; Δ = 1.32 ppm). IR (ATR, cm^{-1}): 3444 (br), 3055(w), 2981 (w), 2927 (w), 2907 (w), 2867 (w), 1601 (m), 1580 (w), 1561 (w), 1474 (w), 1453 (w), 1427 (m), 1392 (w), 1369 (w), 1293 (w), 1247 (m), 1213 (w), 1162 (w), 1097 (m), 1052 (s), 1025 (s), 992 (w), 963 (m), 883 (w), 827 (w), 781 (s), 710 (w), 690 (w), 669 (w).

*DMTPy-O-Benzyl-3-($MePO_3H_2$)-5-($MePO_3HNa$) (**16**, BisPod^{H}):* Crude **15** (57 mg, 0.075 mmol) was dissolved in dry CH_2Cl_2 (2 mL) in a *J Young* Schlenk and TMSBr (280 uL, 2.122 mmol, 28 eq.) was added. The flask was sealed and the slightly yellowish solution was stirred for 15 h at 45 °C under N_2. After removal of all volatiles at HV (using a N_2 trap), dry MeOH (5 mL) was added (to methanolyse the silyl-oxygen bonds) and the mixture was stirred for 3 h at 60 °C. The reaction mixture was concentrated *in vacuo* (180 mbar, 42 °C) and dried at HV. The colourless residue was dissolved in MeOH (very few, so that is was just dissolved) and upon addition of EtOAc (5 mL), the product precipitated as a colourless solid. The latter was isolated by filtration and washed with additional EtOAc (5 mL) and MTBE (5 mL). Crude **16** was purified by Sep-Pak® cartridge (H_2O/MeOH 1:0 to 3:1). The respective fractions were combined, concentrated *in vacuo* (60 mbar, 48 °C) to full dryness and dried at HV to obtain pure product (28 mg, 0.045 mmol, 60 %) as a colourless solid. IR (ATR, neat): 3233 (w), 2059 (w), 3016 (w), 2914 (w), 1630 (w), 1601 (m), 1582 (w), 1560 (w), 1508 (w), 1454 (m), 1429 (m), 1408 (w), 1379 (w), 1299 (w), 1226 (m), 1158 (w), 1122 (w), 1094 (w), 1061 (s), 992 (w), 980 (w), 927 (s), 878 (w), 830 (m), 816 (m), 779 (s), 752 (m), 744 (m), 723 (w), 710 (w), 700 (w), 678 (m), 666 (w). ^{1}H-NMR (400 MHz, MeOD): 8.64 (d, *J* = 4.2 Hz, 1 H); 8.53 (d, *J* = 5.4 Hz, 2 H); 8.31 (d, *J* = 7.6 Hz, 1 H); 8.06 (t, *J* = 8.0 Hz, 2 H); 7.91 – 7.85 (m, 4 H); 7.47 (dd, *J* = 4.9, 0.5 Hz, 2 H); 7.42 (ddd, *J* = 7.4, 4.9, 0.9 Hz, 1 H); 7.16 (s, 2 H); 7.13 (s, 1 H); 4.40 (s, 2 H), 2.97 (d, *J* = 21.3 Hz, 4 H); 2.50 (s, 6 H). ^{31}P-NMR (162 MHz, MeOD) δ= 21.13. UPLC/ESI-MS (r_t = 1.3 min): *m/z* = 324.1 (100, $[M+2H]^{2+}$, 647.1 (15, $[M+H]^+$). Anal. calcd. for $C_{32}H_{31}N_4NaO_7P_2$ + 3.5 H_2O + ⅓ EtOAc (%): C: 52.61, H: 5.39, N: 7.37. Found: C: 52.67, H: 5.33, N: 7.35. HR-ESI-MS (MeOH): 322.08130 (100, $C_{32}H_{30}N_4O_7P_2^{2-}$; $[M-2H]^{2-}$; calc. 322.08003; δ= 3.92 ppm), 645.16703 (22, $C_{32}H_{31}N_4O_7P_2^-$; $[M-H]^-$; calc. 645.16735; Δ = 0.49 ppm), 667.14870 (13, $C_{32}H_{30}N_4NaO_7P_2^-$; $[M-H+Na-H]^-$; calc. 667.14929; Δ = 0.89 ppm).

Synthesis of Co(II) Tetrapyridyl Complexes

The synthesis of *$CoBr_2$(TPy-OH)* **20** was reported earlier.[9]

*[$CoBr_2$(DMTPy-O-Benzyl-3,5-bis($MePO_3Et_2$))] (**20**, Co^{II}BisPod^{Et}):* DMTPy-O-Benzyl-4-$MePO_3Et_2$ (**15**, 19 mg, 0.025 mmol) was dissolved in degassed MeOH (2.5 mL) and dry $CoBr_2$ (36 mg, 0.165 mmol, 6.9 eq.) was added. After the reddish solution was stirred for 30 min at 23 °C under N_2, the mixture was diluted with CH_2Cl_2 (25 mL) and the org. phase was washed with diluted aq. HBr (0.1 M, 3 x 25 mL). Drying of the org. phase over Na_2SO_4, filtration and concentration *in vacuo* (42 °C, 680 mbar) gave pure **21** (21 mg, 0.021 mmol) as pale-red solid in 86% yield. ESI-MS: m/z = 408.7 (7, $[M-2Br]^{2+}$), 898.1 (100, $[M-Br]^+$). Anal. calcd. for $C_{40}H_{48}Br_2CoN_4O_7P_2$ + MeOH + 2.5 H_2O (%): C: 46.69, H: 5.45, N: 5.31. Found: C: 46.61, H: 5.44, N: 5.22. HR-ESI-MS (MeOH): 896.15035 (100, $C_{40}H_{48}O_7N_4BrCoP_2^+$; calc. 896.15081; Δ = 0.51 ppm). IR (ATR, cm^{-1}): 3419 (br), 3070 (w), 2980 (w), 2926 (w), 2070 (w), 2853 (w), 1729 (w), 1608 (m), 1578 (w), 1562 (w), 1447 (m), 1408 (w), 1392 (w), 1369 (w), 1301 (w), 1291 (w), 1246 (m), 1162 (m), 1098 (m), 1084 (w), 1050 (s), 1022 (s), 965 (m), 946 (m), 879 (w), 837 (w), 728 (w), 710 (w), 684 (w), 670 (w), 655 (w).

*The **WRC** [Co(DMTPy-O-Benzyl-3,5-bis($MePO_3H$)] (**22**,Co^{II}BisPod^{H}):* Complex **21** (103 mg, 0.105 mmol) was dissolved in dry CH_2Cl_2 (5 mL) and TMSBr (415 µl, 3.149 mmol, 30 eq.) was added. The red solution was stirred for 15 h at 45 °C under N_2. After removal of all volatiles at HV (using a N_2 trap), dry MeOH (5 mL) was added (to methanolyse the silyl-oxygen bonds) and the mixture was stirred for 3 h at 60 °C under N_2. The reaction mixture was then concentrated to full dryness at HV (using a cooling trap) to obtain crude **22** (**WRC**) (93 mg) as reddish solid. After the red residue was dissolved in H_2O (20 mL) and neutral pH (7) was adjusted by adding diluted aq. Na_2CO_3, the

product was loaded on a Sep-Pak® cartridge for purification. After intensive rinsing with H_2O (40 mL) to remove residual salts, the product was eluted with MeOH (5 mL). The methanolic solution was filtered using a syringe filter (pore size: 25 µm), concentrated *in vacuo* (48 °C, 60 mbar) and dried at HV to obtain pure product **22** (23 mg, 0.033 mmol) as a pink solid in a yield 32%. Crystallization from MeOH yieldedsingle crystals. Anal. calcd. for $C_{32}H_{30}CoN_4O_7P_2$ + MeOH + 2 H_2O (%): C: 51.37, H: 4.96, N: 7.26. Found: C: 51.49, H: 4.98, N: 7.28. HR-ESI-MS (MeOH): 704.09913 (100, $C_{32}H_{30}CoN_4NaO_7P_2^+$; $[M+H]^+$; calc. 704.09945; Δ = 0.63 ppm).

Adsorption of Molecules on Mesoporous Metal Oxides

Samples were prepared by slot coating (doctor-blading) of a ZrO_2 nanoparticle precursor paste (20 nm, Solaronix Zr Nanoxide Z/SP with one layer of Scotch tape on UV-grade CaF_2 windows (Crystran). After heating the samples to 500 °C at a rate on 10 °C/min and sintering them under air at 500 °C for 2 h, they were left to cool down to 60 °C and then the ≈2 µm thick mesoporous films were immersed into MeOH solutions with different molar ratios of **PS** and **WRC**.

Methanolic stock solutions (0.4 mM) of the respective compounds were prepared. An aliquot of the **PS** stock solution (2 mL) was transferred in a jam jar (Ø 4 cm), the corresponding amount of $Co^{II}BisPod^H$ or $BisPod^H$ solution to match the desired ratio was added and the volume was filled up to 4 mL. UV-grade CaF_2 windows (*Crystran*) were doctor-bladed with the corresponding metal oxide paste according to a previously published procedure.[2] Before adsorption of the molecular species, the windows were kept at 60 °C on a hot plate for 30 min and then immersed hot into the respective methanolic solution. After 16 h, the windows were taken out, rinsed with MeOH (5 mL) and dried on the hot plate at 60 °C for 30 min.

Quantification of the Adsorbed Species

By adsorption of the molecules on nanoparticles with known surface area, the size of the footprint of one **WRC** molecule and thus the surface loading could be determined using HPLC methods. After coating NPs with well-defined surface areas (specific surface areas: TiO_2 P25 (Evonic) 50±15 m^2/g; ZrO_2 (US Research Nanomaterials Inc.), 30±10 m^2/g) with the respective molecules the supernatant as well as wash solutions were analysed by the HPLC-3 method to determine the remaining concentrations in comparison to the loading solution. The footprint of the **WRC** was 1.1±0.3 nm^2 on TiO_2 and 2±0.6 nm^2 on ZrO_2, which is rationalized by different M–O distances leading to varying surface densities. For the **PS** we assumed a similar footprint size as for the **WRC** owing to the same number of anchoring substituents.

To determine whether there is a preference towards the adsorption of either of ClRePAbpy (**PS**) and $Co^{II}BisPodH$ (**WRC**) to the metal oxide the methanolic loading solution and the supernatant after adsorption were investigated by *inductively coupled plasma mass spectrometry* (ICP-MS). HPLC analysis failed to determine the respective concentrations due to the exchange of the axial chloride on the **PS** and with this the formation of various Re^I-species. For this, the Re and Co concentration in the loading solution before impregnation of the NP, as well as after

removal of the coated particles, is determined. From this data, the ratio of **PS** and **WRC** *on* the particle can be calculated.

Five methanolic solutions with different ratios of **PS** and **WRC** were prepared (Table S1) and samples for analysis were withdrawn (*loading*). To each solution, equal amounts of ZrO_2 NP were added, and the mixtures were stirred overnight in the dark. After removal of the particles by centrifugation, samples of the methanolic solution were withdrawn for post-adsorption analysis (*supernatant*). All samples were concentrated *in vacuo* to full dryness and after acidic digestion of the solid residue, the Re and Co concentrations in the original solution were determined by ICP-MS. Then, the Re/Co ratios on particle was calculated (Table S1). To validate the ICP-MS procedure, reference samples were measured, and the results were compared to data from elemental analysis. For cobalt, [CoBr(aPPy)]Br[10] was utilized as reference and the concentration determined by ICP-MS data was in good agreement with the expected concentration based on elemental analysis, with ICP-MS values being too low by 6-9%. The chosen reference for rhenium was $(NEt_3)_2[ReBr_3(CO)_3]$, and the results for ICP-MS were too low by up to 13-16% from the values expected from elemental analysis. This disagreement of the elemental analysis and ICP-MS data could originate from the prepared Re-calibration solutions used for concentration determination. While for samples 1–3 between 24 and 28% of the available molecules were adsorbed, in case of the equimolar **PS**/**WRC** mixture (sample 4), 52% of **PS** and 44% of **WRC** were adsorbed to the same surface area, which results in a higher coverage density on the particles. This observation is attributed to the fact, that the cobalt complex has a long linking group situating the cobalt center further away from the surface compared to the rhenium complex, which is located very close to the surface. With this layered architecture, a higher molecule loading is achieved compared to composites with only a single immobilized species or the higher overall concentration of the loading solution.

Even though sample 1 and 5 never were in contact with either cobalt or rhenium, ICP-MS measurements still indicated the presence of the respective metal. The corresponding values were therefore considered as baseline of the measurement and with this as minimal error. Table S1 shows that within the margin of experimental error the ratio of **PS**/**WRC** on the surface is the same as in the loading solution with a deviation of 10-15%.

Table S1 *Target and measured ratios of loading solution, determined ratios of supernatants as well as calculated adsorbed ratios from ICP-MS measurements.*

sample	target ratio[a]	loading[b]		supernatant[b]		adsorbed[c]	
	Re:Co	Re:Co		Re:Co		Re:Co	
1	100:0	100.0	0.3	100.0	0.4	100.0	0.2
2	100:1	100.0	0.3	100.0	0.4	100.0	0.2
3	100:10	100.0	2.8	100.0	1.0	100.0	8.7
4	100:100	100.0	101.8	100.0	120.2	100.0	85.2
5	0:100	0.1	100.0	0.1	100.0	0.2	100.0
[a] loading ratio aimed for, [b] ratio determined by ICP-MS, [c] ratio calculated from measurement data							

Time Resolved Measurements

Experimental Methods

Transient IR spectroscopy: The main method of investigation was transient IR spectroscopy. The tr-IR spectrometer consists of two amplified Ti:sapphire lasers at 2.5 kHz that are electronically synchronized. This allows for pump–probe delay times from ≈10 ps to ≈40 µs, where the lower resolution limit is caused by the jitter of this electronic synchronization.[11] The excitation pulses were centered at 400 nm for the measurements on ZrO_2. They were obtained by frequency doubling of the first Ti:sapphire laser. Mid-IR probe pulses were generated from the second Ti:sapphire laser in a tunable home-built OPA.[12] After the sample the probe pulses were dispersed in a spectrograph and detected using a 2×64 pixel MCT detector that covers a 200 cm^{-1} spectral window with ≈ 4 cm^{-1} resolution. The pump pulses were stretched to 4 ps and the laser fluency was kept below 60 µJ/cm^{-2} at which excitation density is low enough to rule out triplet-triplet annihilation. This results in tr-IR signals usually lower than 1mOD for the CO stretch modes. To ensure long term stability of the samples they were constantly moved during data acquisition using a home-built 2D raster scanner. Ar purged ethanol or D_2O were used as solvents.

Transient Vis spectroscopy: For the transient Vis measurements, in essence the same laser system described above was used, except for the visible probe pulses, which were generated by tightly focusing ca. 1 µJ of the 800 nm pulses into a stationary 3 mm thick sapphire plate. After passing the sample, the probe beam was collimated, dispersed by a UV transmission grating (Thorlabs, 830 l mm^{-1}), focused by a 75 mm fused silica lenses onto a 2048-pixel CMOS line array (Synertronic Designs). The probe spectral axis was calibrated by fitting the position of the transmission maxima of several interference filters, and the light intensity was controlled by using broadband neutral density filters to prevent saturation of the detector. Colour-balancing filters were used to homogenise the light intensity profile of the probe and reference beams. The obtained spectral resolution was ca. 0.8 nm after binning of four adjacent pixels to improve the signal-to-noise ratio, yielding 512 effective pixels.

Pump-probe difference spectra were obtained by alternately blocking consecutive pump laser shots using a mechanical chopper. The pump beam polarisation was set to magic angle with respect to the probe. The sample was raster-scanned during the course of the measurement to ensure proper sample exchange between laser shots.

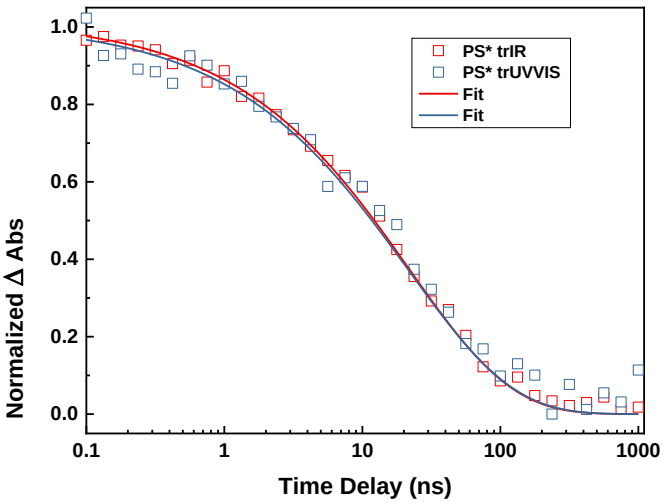

*Figure S*1. Comparison of the **PS*** excited state kinetics as obtained from the tr-IR and the tr-Vis measurement.

To compare the transient Vis data with the tr-IR data, it was crucial to match the excitation density of both experiments. We confirmed that we measure the same kinetics for the excited state relaxation of **PS*** on the ZrO_2 surface to make sure that all subsequent reaction steps will be comparable between the two experiments (Fig. S1). This however resulted in rather small signal intensities for the tr-Vis measurement.

tr-IR Results

Contour plots for tr-IR measurements of **PS** and **2** are shown in Figure S2 and S3. The top row shows the tr-IR spectra in the absence of the **ED** with increasing x_{WRC} from left to right. Compound **2** (Fig. S3) has an additional -NCS band at ≈2110 cm^{-1} that shifts in the opposite direction to the -C≡O bands in ^{3}**PS*** and **PS**$^-$**,** but can also be used as an indication for the formation of reduced state **PS**$^-$. The lowest energy optical excited state of **2** has been shown to be a mixed LLCT/MLCT state, so electron density is withdrawn from the -NCS ligand thus changing its vibrational energy.[13] Spectral overlap of the –NCS* vibrational mode of **2*** with the a'(1)* ν_{CO} mode makes the comparison with **PS**, where this cannot occur, indispensable for a conclusive interpretation of the transient data for **2**. A selected transient IR spectra of **PS** is shown in Fig. 2 in the main manuscript as example and further reference for the ground state bleach of **PS** as well as the vibrational modes bands assigned to the ^{3}**PS*** triplet excited state absorption and the reduced photosensitizer **PS**$^-$.

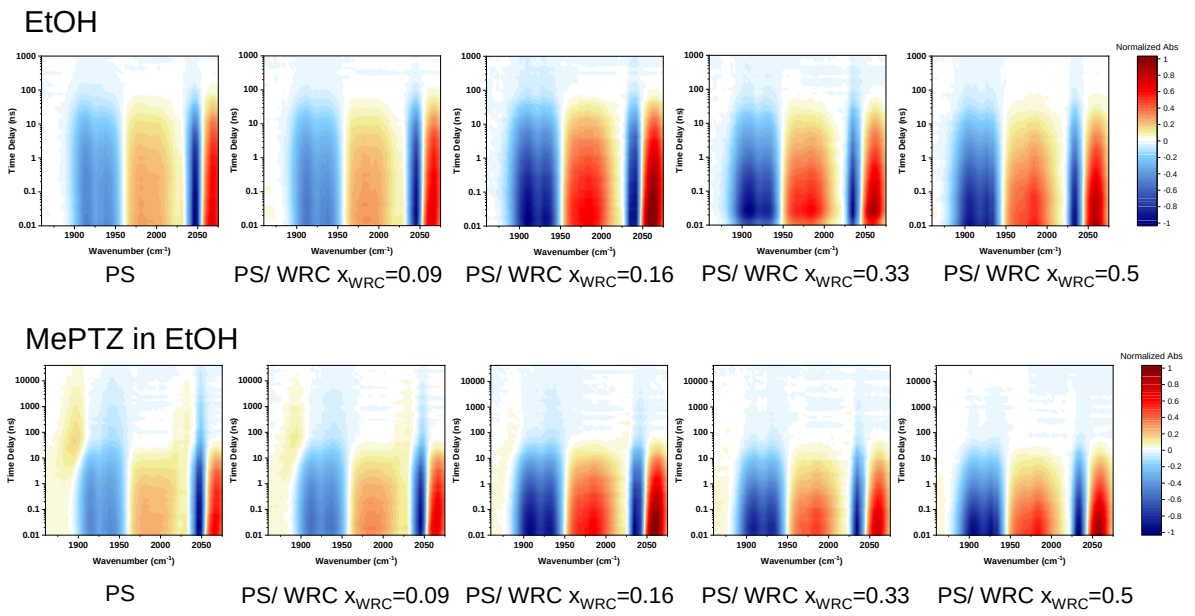

Figure S2. Normalized tr-IR data of **PS** on ZrO_2 with different ratios of **PS/WRC** in contact with EtOH (top row) and 50 mM MePTZ in EtOH as a quencher (bottom row)

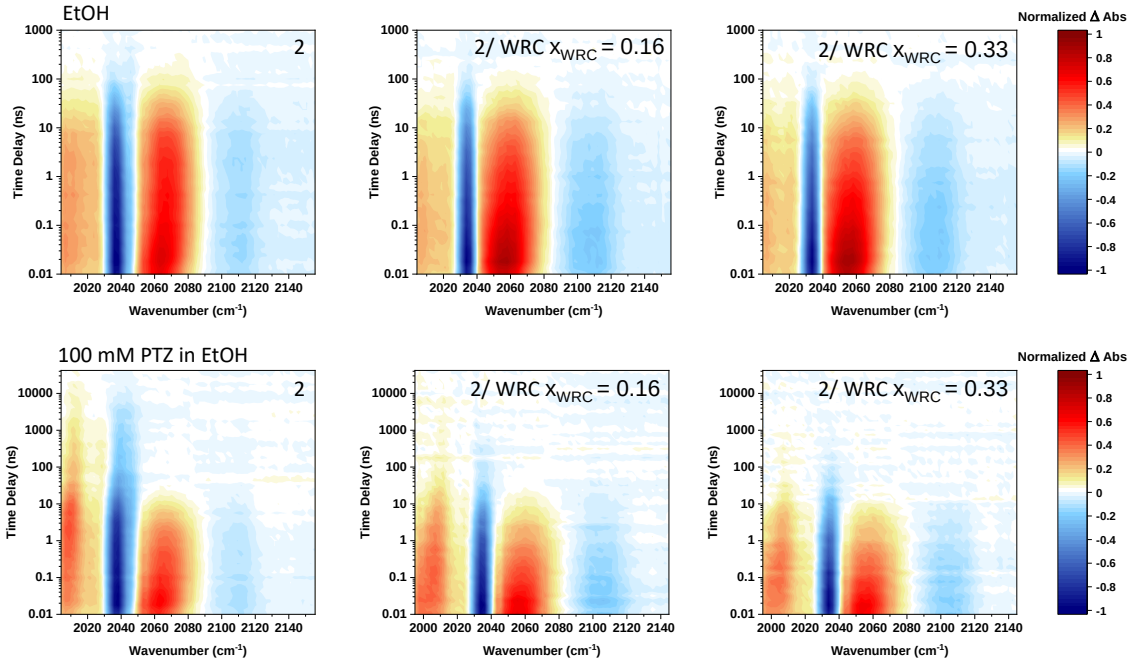

Figure S3. Normalized tr-IR data of photosensitizer **2** on ZrO_2 with different ratios of photosensitizer **2/WRC** and ethanol (top row), resp. 100 mM 10H-phenothiazine in ethanol as a quencher (bottom row)

Going from a more stable organic solvent to an aqueous solution in contact with the sensitized ZrO_2 surface we considered the possibility that the chloride ligand of the adsorbed **PS** will exchange for D_2O to form the aquo-complex, hence the very short excited state lifetime of **PS** on ZrO_2 in comparison to **PS** previously mentioned. The -NCS ligand of **2** has been shown to be stable under steady state irradiation conditions in the presence of an **ED** and a **WRC**[13] but also shows a large decrease in the excited state lifetime in contact with D_2O both at the surface and in solution (Table S2). We assume that over the course of the tr-IR measurement **PS** is stable enough, not only in EtOH but also in water, because we did not observe scan to scan spectral shifts in the transient spectra and changes of smaller than 10% in signal intensity. In Fig. S4a we show the transient IR spectra of **PS** on ZrO_2 with D_2O and 1M equimolar ascorbate/ ascorbic acid as electron donor with a sample of **PS** and **WRC** (x_{WRC}=0.09) measured under the same conditions Fig. S4b.

Table S2. Excited state lifetimes of the photosensitizers in solution and on ZrO_2 with D_2O and EtOH. For surface immobilized molecules a stretched exponential fitting function has been applied, with the stretching parameter β set to 0.55 to compare between samples. The average lifetimes were calculated as $\langle\tau\rangle=\tau/\beta\ \Gamma(1/\beta)$ (with the gamma function Γ).

PS	**τ_{em} in EtOH[a]**	**$\langle\tau\rangle$ on ZrO_2 with EtOH**	**τ_{em} in H_2O[b]**	**$\langle\tau\rangle$ on ZrO_2 with D_2O**
PS	20.1 ns	38±2 ns	3 ns	8.1±0.3 ns
2	104 ns	24±4 ns	18.8±0.4 ns	-

[a] Luminescence lifetime samples had a concentration of 0.1 mM in degassed ethanol λ_{exc}=371.1 nm, λ_{em}=600 nm; [b] Samples 0.1 mM in degassed water, λ_{exc}=371.1 nm, λ_{em}=600 nm.

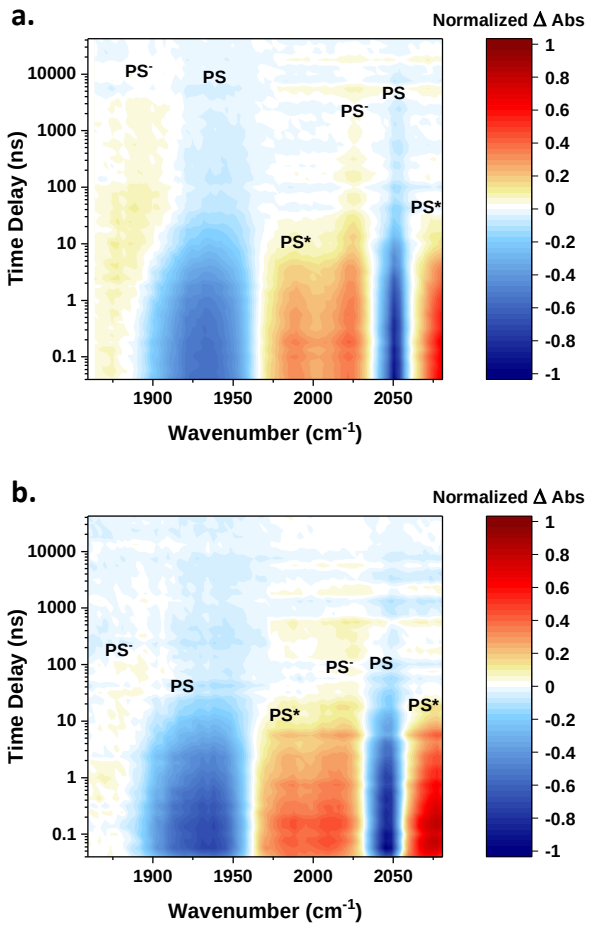

Figure S4. (a) tr-IR contour plot of **PS** on ZrO_2 with 1M HAsc/Asc^- 1:1 as ED. (b) tr-IR contour plot of **PS/WRC** (x_{WRC}≈0.1) on ZrO_2 with 1M HAsc/Asc^- 1:1 as **ED**.

FT-IR Measurements

In Fig. S5 the FTIR spectra of both photosensitizers **1 (PS)** (in Fig. S5a) and **2** (in Fig. S5b) on ZrO_2 are plotted. Mixtures of photosensitizer and **WRC** or photosensitizer and ligand **16** adsorbed on the same substrate are also shown. Small changes in the integrated FTIR absorbance can be attributed to differences in thickness of the oxide layer. For comparison spectra of the **WRC** alone on ZrO_2 and a ZrO_2 background are also given in Fig. S5a and S5b. The **WRC** is characterized by an absorption at 1606-1610 cm^{-1} that is hardly shifting in presence of the photosensitizers. The same applies to the vibrational mode of the photosensitizers at 1399 cm^{-1} that is unaffected by the presence of the **WRC**. The carbonyl modes of both photosensitizers shift to lower energy in presence of **WRC** or ligand **16**. It is also remarkable that the -NCS mode of **2** experiences a red shift in the presence of the **WRC** similar to the CO bands. This indicates that the interaction is not a formal reduction of the photosensitizer, which would lead to a blue shift of the ν_{NCS} modes as has been shown in[13] and an opposite red shift of the ν_{CO} bands. This can also be seen by the weak ν_{NCS} band of reduced **2** in presence of phenothiazine as electron donor at ≈2140 cm^{-1} in

Fig. S3 (bottom left). The effect can be attributed to a combination of the influence from the ligand environment and the presence of the 2+ charge on the **WRC**. This was shown by the measurement of only the ligand **16** (without cobalt) co-adsorbed with **PS** (x_{16}=0.5), where this effect is still present, but slightly smaller (Fig. S5a, yellow curve).

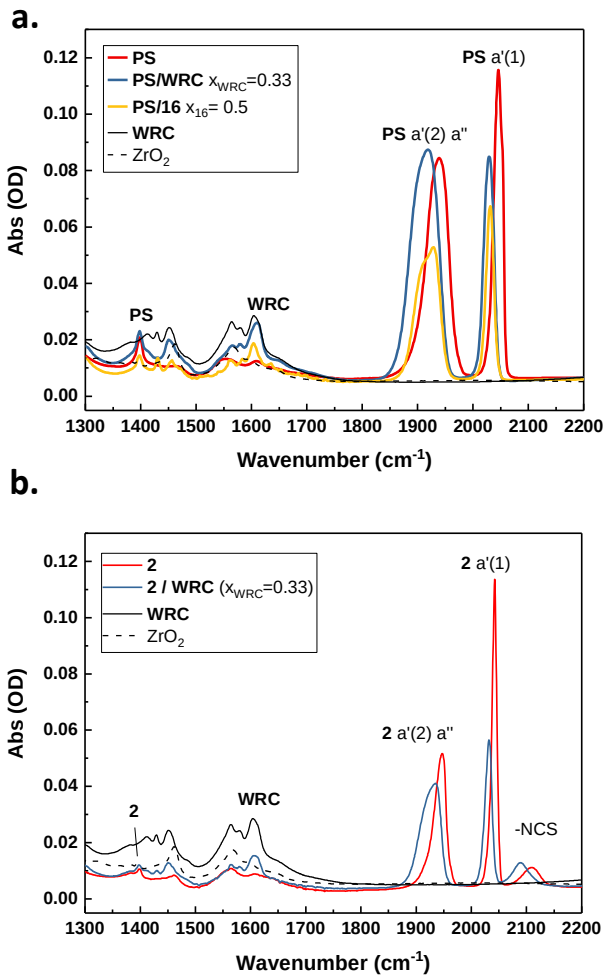

Figure S5. (a) FTIR spectra of **PS** on ZrO_2 with (violet trace) and without (red) co-adsorbed **WRC**, as well as the **WRC** on ZrO_2 alone (black) and a ZrO_2 background (dashed) for comparison and **PS** co-adsorbed with only the ligand (**16**) of the **WRC** (yellow curve). (b) FTIR spectra of photosensitizer **2** ([Re^{I}NCS)(CO)$_3$(2,2'-bipyridine-4,4'-bisphosphonate)]) on ZrO_2 with (blue) and without (red) co-adsorbed **WRC** as well as the **WRC** on ZrO_2 alone (black) and ZrO_2 (dashed).

Electrochemical Measurements

Fig S 6a shows the cyclic voltammetry (CV) and differential pulse voltammetry (DP) of **20** Co Br_2 (Tpy-OH) (1 mM) in water with 100 mM lithium trifluoromethanesulfonate on a glassy carbon working electrode, Pt auxiliary electrode and a Ag/AgCl reference electrode. $K_3[Fe(CN)_6]$ at +430 mV vs. NHE was used as internal standard.[14] The oxidation from Co^{II}/Co^{III} is irreversible with the anodic and cathodic peak potentials of E_{pa} = 0.76 V and E_{pc} = 0.53 V vs. NHE. The reduction is followed by a typical wave for electrode grafting upon reoxidation, this the half wave potential was determined from differential pulse voltammetry and was found to be $E_{1/2}$ = -0.97 V vs. NHE.

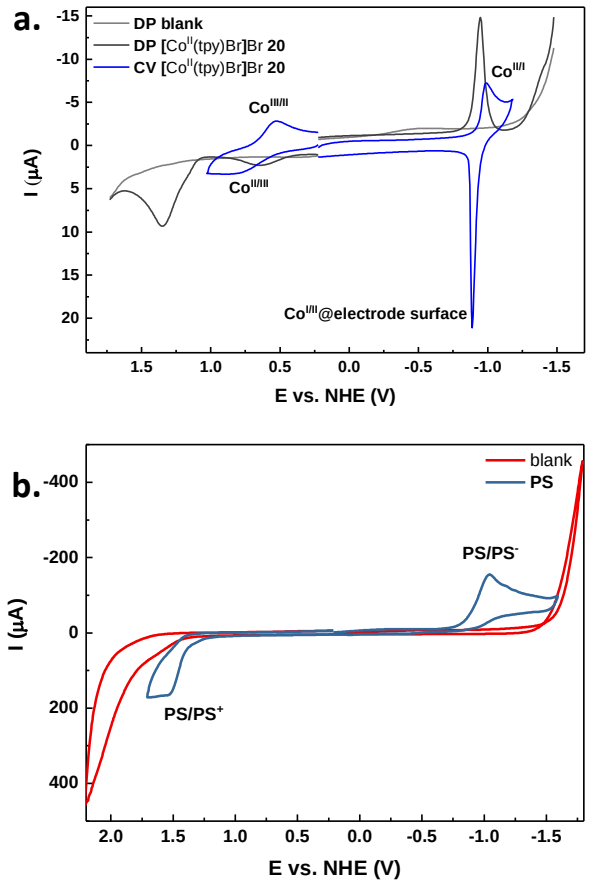

Figure S6. (a) Cyclic voltammetry (CV) and differential pulse voltammetry (DP) of **20** (b) Cyclic voltammetry of **PS**

Fig. S6b shows the cyclic voltammogramm of **PS** (3mM). It was measured in 0.1 M KCl at a glassy carbon working electrode, with a Pt wire auxiliary electrode and a Ag/AgCl/3M NaCl reference electrode with a reference potential of +209 mV vs. NHE as reported by the manufacturer (BASI). Both oxidation and reduction are irreversible with E_{pa} = +1.55 V and E_{pc} = -1.04 V vs. NHE, respectively.

References

(1) Krejčik, M.; Daněk, M.; Hartl, F. Simple Construction of an Infrared Optically Transparent Thin-Layer Electrochemical Cell. *J. Electroanal. Chem. Interfacial Electrochem.* **1991**, *317* (1–2), 179–187. https://doi.org/10.1016/0022-0728(91)85012-E.

(2) Oppelt, K.; Fernández-Terán, R.; Pfister, R.; Hamm, P. Geminate Recombination versus Cage Escape in the Reductive Quenching of a Re(I) Carbonyl Complex on Mesoporous ZrO2. *J. Phys. Chem. C* **2019**, *123* (32), 19952–19961. https://doi.org/10.1021/acs.jpcc.9b04950.

(3) Zabka, W.-D.; Musso, T.; Mosberger, M.; Novotny, Z.; Totani, R.; Iannuzzi, M.; Probst, B.; Alberto, R.; Osterwalder, J. Comparative Study of the Different Anchoring of Organometallic Dyes on Ultrathin Alumina. *J. Phys. Chem. C* **2019**, *123* (36), 22250–22260. https://doi.org/10.1021/acs.jpcc.9b05209.

(4) Markovac, A.; LaMontagne, M. P. Antimalarials. 12. Preparation of Carbon Isosteres of Selected 4-Pyridinemethanols as Suppressive Antimalarials. *J. Med. Chem.* **1980**, *23* (11), 1198–1201. https://doi.org/10.1021/jm00185a009.

(5) Ghobril, C.; Popa, G.; Parat, A.; Billotey, C.; Taleb, J.; Bonazza, P.; Begin-Colin, S.; Felder-Flesch, D. A Bisphosphonate Tweezers and Clickable PEGylated PAMAM Dendrons for the Preparation of Functional Iron Oxide Nanoparticles Displaying Renal and Hepatobiliary Elimination. *Chem. Commun.* **2013**, *49* (80), 9158–9160. https://doi.org/10.1039/c3cc43161d.

(6) Collman, J. P.; Zhong, M.; Wang, Z.; Rapta, M.; Rose, E. Efficient Synthesis of a Porphyrin−N-Tripod Conjugate with Covalently Linked Proximal Ligand: Toward New-Generation Active-Site Models of Cytochrome c Oxidase. *Org. Lett.* **1999**, *1* (13), 2121–2124. https://doi.org/10.1021/ol9911730.

(7) Cooray, N. F.; Tsukada, M.; Wakamura, M.; Anazawa, T.; Matsuura, A.; Sato, H. The Organic Pigment, and Photosensitive Element. JP6056605, 2017.

(8) Batesky, D. C.; Goldfogel, M. J.; Weix, D. J. Removal of Triphenylphosphine Oxide by Precipitation with Zinc Chloride in Polar Solvents. *J. Org. Chem.* **2017**, *82* (19), 9931–9936. https://doi.org/10.1021/acs.joc.7b00459.

(9) Guttentag, M.; Rodenberg, A.; Bachmann, C.; Senn, A.; Hamm, P.; Alberto, R. A Highly Stable Polypyridyl-Based Cobalt Catalyst for Homo- and Heterogeneous Photocatalytic Water Reduction. *Dalt. Trans.* **2013**, *42* (2), 334–337. https://doi.org/10.1039/C2DT31699D.

(10) Schnidrig, S.; Bachmann, C.; Müller, P.; Weder, N.; Spingler, B.; Joliat-Wick, E.; Mosberger, M.; Windisch, J.; Alberto, R.; Probst, B. Structure–Activity and Stability Relationships for Cobalt Polypyridyl-Based Hydrogen-Evolving Catalysts in Water. *ChemSusChem* **2017**, *10* (22), 4570–4580. https://doi.org/10.1002/cssc.201701511.

(11) Bredenbeck, J.; Helbing, J.; Hamm, P. Continuous Scanning from Picoseconds to Microseconds in Time Resolved Linear and Nonlinear Spectroscopy. *Rev. Sci. Instrum.* **2004**, *75* (11), 4462–4466. https://doi.org/10.1063/1.1793891.

(12) Hamm, P.; Kaindl, R. A.; Stenger, J. Noise Suppression in Femtosecond Mid-Infrared Light Sources. *Opt. Lett.* **2000**, *25* (24), 1798–1800. https://doi.org/10.1364/OL.25.001798.

(13) Probst, B.; Rodenberg, A.; Guttentag, M.; Hamm, P.; Alberto, R. A Highly Stable Rhenium−Cobalt System for Photocatalytic H 2 Production: Unraveling the Performance-Limiting Steps. *Inorg. Chem.* **2010**, *49* (14),

6453–6460. https://doi.org/10.1021/ic100036v.

(14) Dutton, P. L. Redox Potentiometry: Determination of Midpoint Potentials of Oxidation-Reduction Components of Biological Electron-Transfer Systems. In *Methods in Enzymology*; Colowick, S. P., O., K. N., Eds.; Academic Press, Inc.: New York, 1978; Vol. LIV, pp 421–423.